13. The Effect of Whipping Stress on Fatigue Strength of a Fast Container Ship in Rough Seas

Yoichi SUMI*, *Member*, Yoshiyuki YAMAMOTO**, *Member*, Masanao SUZUKI***, *Member*

(From J.S.N.A. Japan, Vol. 163, June. 1988)

Summary

It has recently been recognized that structural failures of ocean–going vessels in rough seas are closely related to the dynamic hull girder stresses induced by slamming impact and by nonlinear dynamical forces acting on bow flare. In the present paper, fatigue strength of a container ship is investigated for structural members with high stress concentration factors, where the applied stress is composed of wave induced bending stresses including nonlinear effects and whipping stresses. Having calculated the dynamic stresses arising in a hull girder in rough seas, fatigue strength of highly stressed portions is examined by using appropriate S–N curves. When a high speed vessel passes through rough seas, it is found that the significant increase of the repeated stress ranges due to the superposed whipping component of stresses may drastically reduce the fatigue life of highly stressed structural members.

1. Introduction

Recent developments in ship structural mechanics have revealed the mechanisms of the hull girder structural failures of ocean–going vessels in rough seas. In head sea conditions nonlinear and dynamic wave forces induce excessive bending moment in the fore body of a hull girder, which may cause the deck buckling and collapse[1),2)], while in oblique waves the excessive torsional moment may be induced, where the corresponding warping stresses cause deck buckling on one side of the deck and also cause cracking failures on the other side in the fore body of a ship[3)]. Local structural failures of stiffened panels such as permanent sets of plates and cracking failures of stiffeners are investigated in relation to the excessive water pressure acting on the panels due to slamming[4)]. The repeated slamming loads also cause corrosion fatigue of materials which may lead to the entire fracture of the bow structure of a ship[5),6)].

* Department of Naval Architecture and Ocean Engineering, Yokohama National University
** Tokyo Denki University
*** Ishikawajima–Harima Heavy Industries Co., Ltd.

After a high speed vessel passes through a rough sea, fatigue cracks are sometimes observed even in the middle and aft parts of a hull girder, where the hull girder bending stress may be magnified by severe stress concentration factors. The highly concentrated stresses are expected to occur at the parts of structures with geometrical discontinuity such as hatch corners and end parts of superstructures. Since some newly built ships have even experienced such damage, the cracking failure might not be explained without taking into account of the dynamically induced whipping stresses superposed on the wave induced stresses.

In the present paper, the initiation of the low–cycle fatigue cracks is investigated by considering wave induced bending stresses with nonlinear effects, whipping stresses of a hull girder, and coupled vibratory stresses of a hull girder and a superstructure. The nonlinear and dynamic stress calculations are performed for an ocean–going container ship with various ship speeds and wave heights. Considering the stress concentration factors and typical S–N curves, the low–cycle fatigue strength is examined based on the calculated stress ranges

including the whipping components which are affected not only by wave heights but also by ship speeds. In order to prevent local fatigue damage for a given period of time, the maximum ship speeds are predicted for various conditions of significant wave heights and stress concentration factors. The numerical results also indicate that the whipping components of stresses cannot be disregarded even in the aft body, while the bending stresses with nonlinear effects are significant only in the fore body.

2. Dynamic Nonlinear Response Analysis of a Fast Container Ship in Regular Water Waves

2.1 A fast container ship and its structural idealization

Numerical calculations are performed for a container ship, whose principal particulars and body plan are shown in Table 1 and Fig. 1, respectively. The moment of inertia of section, I, the shear area, A_s, and weight per unit length, w, which are used as the basic data for the dynamic anlysis of the hull girder, are illustrated in Fig. 2. Since the length and the height of the superstructure are of the same order, it is simply modeled as a shear beam. According to the structural modeling illustrated in Fig. 3,

Table 1 Principal particulars of a container ship

L	: Length between perpendiculars	245.0m
B	: Breadth moulded	32.2m
D	: Depth moulded	24.0m
d	: Draft	11.0m
C_b	: Block coefficient	0.57
W	: Displacement	51,000ton

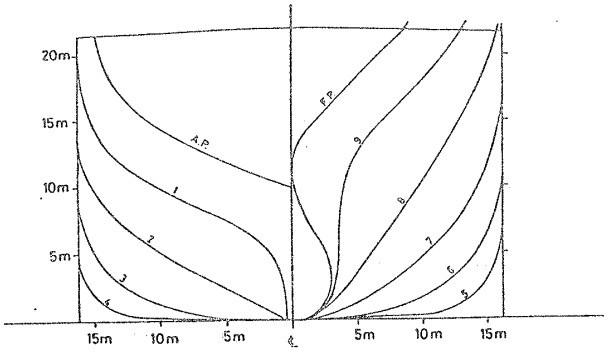

Fig. 1 Body plan of a container ship

the equivalent concentrated mass of the i–th deck is empirically given as

$$m_i = 250 b_i l_i \ (\mathrm{kg}), \tag{1}$$

where b_i (m) and l_i (m) are the breadth and length of the i–th deck, respectively. The shear rigidity between the i–th and (i+1)–th decks is given by

$$k_i = GA_s/h_i, \tag{2}$$

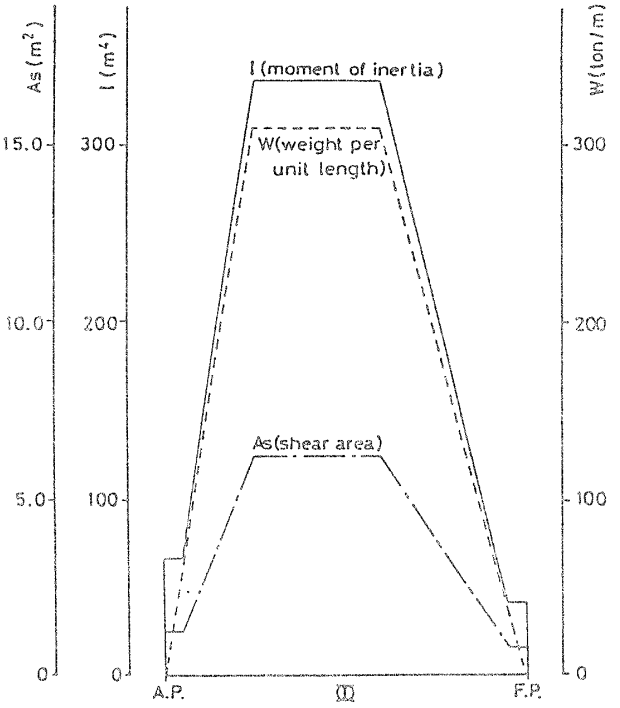

Fig. 2 Distribution of weight, moment of inertia, and shear area of a container ship

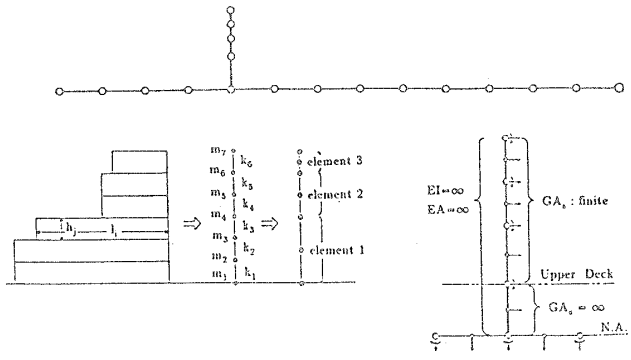

Fig. 3 Structural modeling of a container ship ; overall modeling (top) and modeling of a superstructure (bottom)

where G, A_s, and h_i are the shear modulus, shear area, and the height between the i−th and (i+1)−th decks[7].

In order to approximate the shear deformation of the structure, the hull girder and the superstructure are modeled by Timoshenko beam elements, which have two degrees of freedom at both ends and one degree of freedom at the mid point nodes[8]. The main hull girder structure is divided into 40 elements and the superstructure, whose weight is 700 ton, is divided into three elements. As is illustrated in Fig. 3, the bottom part of the superstructure is connected by a rigid element to the hull girder beam element lined along the nuetral axis of the hull girder. The Young's modulus and shear modulus are chosen as 21,000 kgf/mm^2 and 8,100 kgf/mm^2, respectively. Following the data for similar container ships[9], the logarithmic decrement is assumed as 0.056 in the present analysis.

2.2 Eigen modes of vibration in still water

The eigen frequencies of the hull girder in still water are calculated and the results are listed in Table 2 for the cases both with and without the superstructure. The corresponding modes of vibration are illustrated in Fig. 4, in which the coupled vibration of hull girder and superstructure is observed in the vibration modes with more than six nodes. The main vibration mode of the superstructure has its eigen frequency between the eigen frequencies

Table 2 Natural periods and frequencies of a container ship

number of nodes	hull girder without superstructure period (sec.)	hull girder without superstructure frequency (cpm)	hull girder with superstructure period (sec.)	hull girder with superstructure frequency (cpm)	superstructure period (sec.)	superstructure frequency (cpm)
0	8.903	6.74	8.903	6.74		
1	8.091	7.42	8.093	7.41		
2	1.027	58.44	1.028	58.39		
3	0.453	132.42	0.453	132.41		
4	0.269	222.93	0.269	222.74		
5	0.185	325.19	0.185	324.51		
6	0.138	435.06	0.138	434.91		
7	0.109	548.90	0.109	548.40		
8	0.090	661.50	0.091	662.46		
9	0.077	782.09	0.077	781.32		
10	0.067	899.09	0.067	898.44		
11	0.059	1015.26	0.060	1009.00		
12	0.053	1131.87	0.054	1122.14		
①					0.051	1166.64
13	0.048	1247.61	0.048	1248.27		

N.B.: 0- and 1-node correspond respectively to heaving and pitching motion.

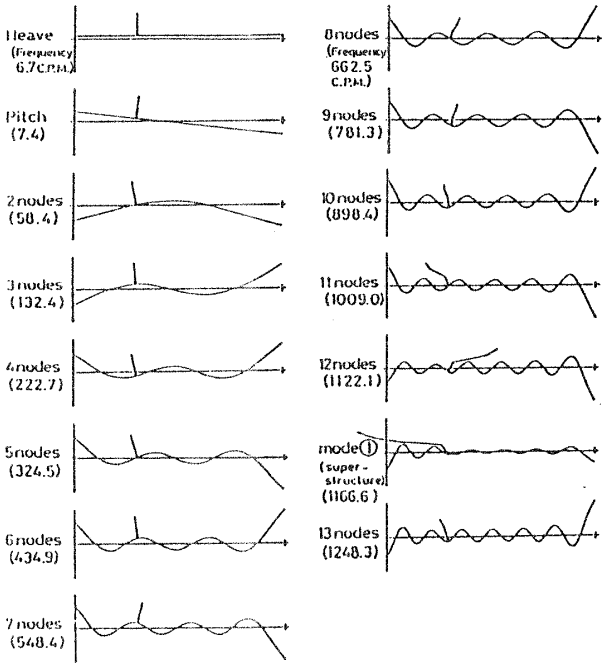

Fig. 4 Eigen modes of vibration of a container ship

corresponding to the hull girder vibration modes of 12−node and 13−node. Although the higher order modes of longitudinal bending vibration are in general coupled with the transverse modes of vibration, these coupling effects are disregarded in the present analysis.

2.3 Wave induced bending moment including whipping effects

In order to investigate the seakeeping performance, experimental measurements had been carried out by using an actual fast container ship, whose recorded speeds were in the range of 15−30 knots depending on the severity of sea states[10]. According to the information given in Ref. [10], the calculation conditions are parametrically selected for the wave heights 6, 8, 10, and 12m and for the ship speeds 6, 10, 14, 18, 22, and 26 knots, respectively, keeping the wave length−ship length ratio as unity.

The Newmark β method is employed for the direct time intergration, while the first four eigen modes, which consist of two rigid motions and two elastic vibration modes with 2 and 3 nodes, are selected as the generalized coordinates for the space discretization. Although the

equation of motion is integrated for six periods of wave encounters, the last two periods are used for the calculation of slamming and whipping stresses in order to avoid trangent behavior of ship motion. Vibratory stresses are also damped for the first four periods by choosing excessive artificial damping coefficient. Considering the frequencies of elastic vibration of the hull girder, the standard step of time integration is chosen as 1/300 of the period of a wave encounter. When considering the coupled vibration of the superstructure and the hull girder, the generalized coordinates are selected up to the 13-node vibration mode, where the time step is chosen as 1/2000 of the period of a wave encounter.

Figures 5–8 show the envelopes of the maximum bending moment of the hull girder, where the discontinuity of the moment at the intersection of the hull girder and the superstructure is less than one percent of the hull girder bending moment and thus can be disregarded. As can be seen from the figures, the sagging moment is significantly increased with the increase of the ship speed due to the effects of slamming followed by whipping. In the case of rigid body calculations, it is shown in Ref.

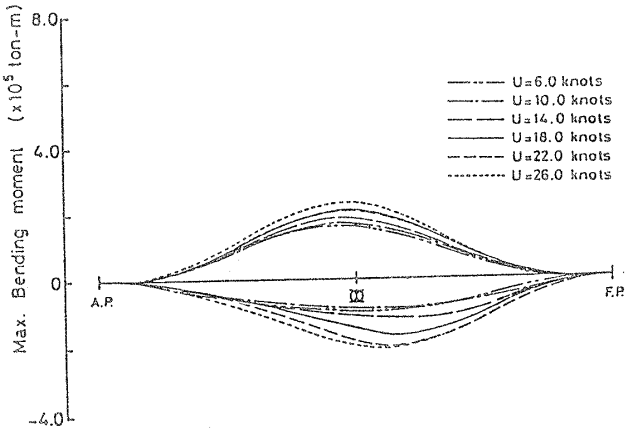

Fig. 5 Longitudinal distribution of maximum bending moment including whipping components (H_w= 6.0m)

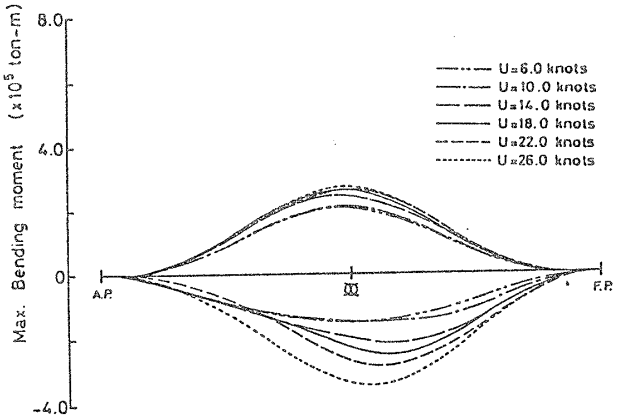

Fig. 6 Longitudinal distribution of maximum bending moment including whipping components (H_w= 8.0m)

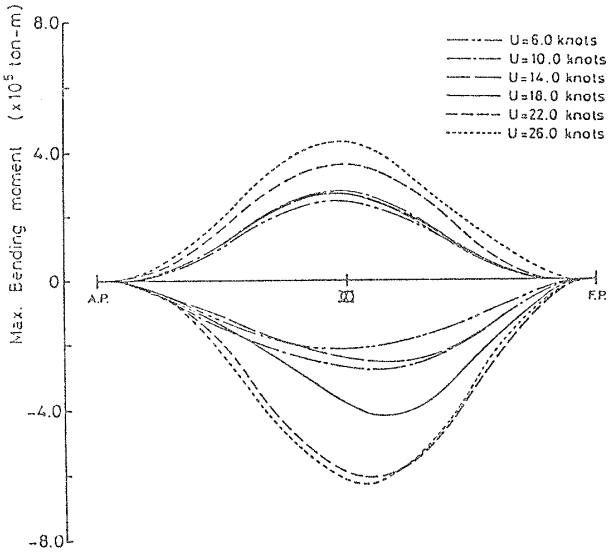

Fig. 7 Longitudinal distribution of maximum bending moment including whipping components (H_w= 10.0m)

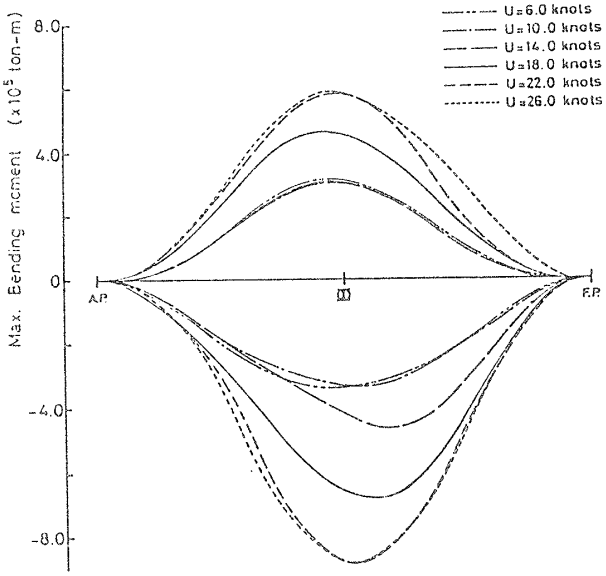

Fig. 8 Longitudinal distribution of maximum bending moment including whipping components (H_w= 12.0m)

[11] that the effects of nonlinear wave forces mainly increase the sagging moment in the fore body of the hull girder. It should be contrasted in the present whipping analysis that the hogging moment is also increased with increasing the ship speed and that the bending moment is increased even in the aft body. As far as the fatigue strength is concerned, the present results suggest the effects of slamming followed by whipping are not localized to the fore body, because a slight increase of stress amplitude remarkably reduces the fatigue life of structural members.

Considerations are made on time histories of hull girder bending moment at S.S. 3–1/2, which is usually located close to the front end of the superstructure and aft end of the hold part where structural discontinuity is often observed. Figure 9 shows the time history of the bending moment and the deck stress for the wave height H_w=6m and ship speed U=6knots. In the case where the wave height is less than six meters, bottom slamming cannot be expected to occur for all ship speeds. On the contrary if the wave height is increased more than eight meters, the bottom emergence could occur. The time histories illustrated in Figs. 10 and 11 indicate that the whipping stress is induced mainly by the nonlinear wave force acting on the bow flare during its immersion rather than by the bottom slamming force. Comparing Figs. 9–11 with each other, it is well recognized that the whipping component is significantly increased with the increases of the ship speed and the wave height. In these figures the duration of the bottom slamming is indicated by a rectangular notation.

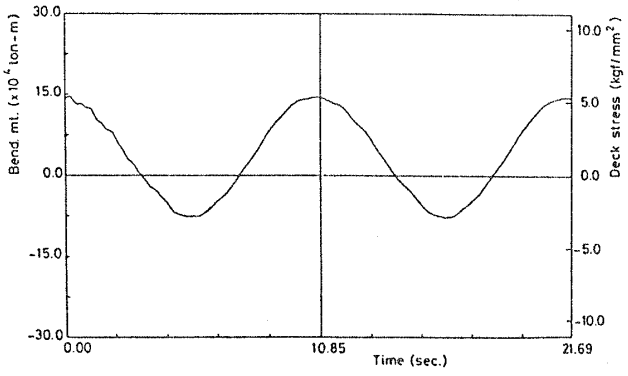

Fig. 9 Time history of bending moment at S.S. 3–1/2 (H_w=6.0m, U=6.0knots)

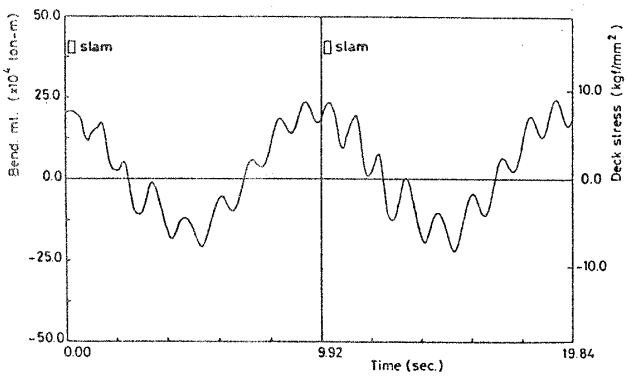

Fig. 10 Time history of bending moment at S.S. 3–1/2 (H_w=10.0m, U=10.0knots)

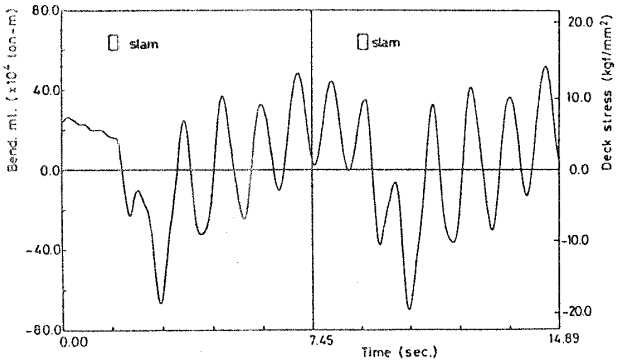

Fig. 11 Time history of bending moment at S.S. 3–1/2 (H_w=12.0m, U=26.0knots)

The vibration of the superstructure due to whipping and the resulting shear stresses in the side walls are investigated for the wave height 8m and a ship speed 18knots, where all eigen modes illustrated in Fig. 4 are included in the analysis. As is shown in Fig. 12, higher order shear vibration which approximately corresponds to the 7–node mode of the hull girder vibration continues for a second just after the bottom slamming. After the higher mode vibration is damped, the superstructure oscillates with the frequency corresponding to the 2–node mode of the hull girder vibration. Since the corresponding values of the shear stresses are of the order of 0.1kgf/mm^2 in the side wall, it is shown in the present analysis that although the vibration of the superstructure may cause discomfort of crew, it can be disregarded from the view point of fatigue strength. It should also be noted that the

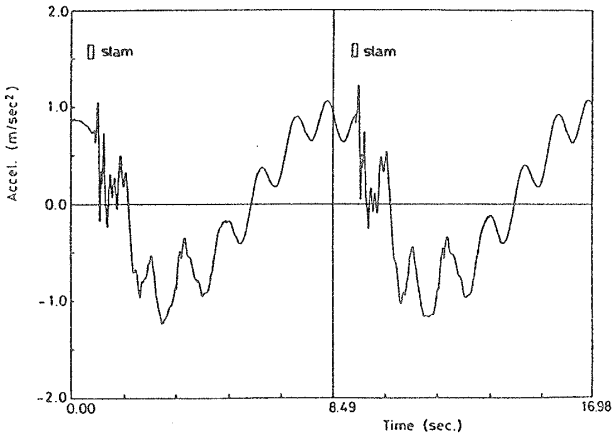

Fig. 12 Time history of longitudinal acceleration at navigation deck (H_w=8.0m, U=18.0knots)

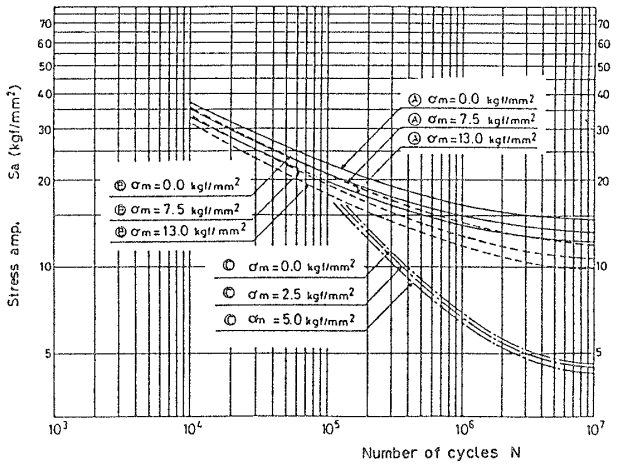

Fig. 13 S–N curves, in which Ⓐ, Ⓑ, and Ⓒ represent each fatigue curve for gas cut surface, continuous fillet weld loaded in weld direction, and cross–shaped fillet weld loaded perpendicular to weld direction

frequency of the higher order vibration observed in the superstructure is lower than its eigen frequency.

3. Fatigue Strength of Structural Members with Stress Concentration

3.1 Estimation of the fatigue damage per a cycle of wave encounter

In case where the hull girder is subjected to slamming followed by whipping, fatigue strength of structural members with high stress concentration factors is examined based on the dynamic stress analysis presented in the previous section and appropriate S–N data. Figure 13 shows the S–N curves used in the present analysis[12], which are applicable for gas cut surface, continuous fillet weld loaded in the weld direction, and cross–shaped fillet weld loaded perpendicular to the weld direction. Taking into account of mean stresses, the S–N curves can be used for not only tension–tension but also tension–compression loading conditions.

Although the definitions of the cycle count of fatigue loading are seriously discussed for the case of complex stress time histories, a fatigue cycle is simply defined to be identical to a cycle of wave encounter in the present analysis, where the stress range is the difference of maximum and minimum bending stresses including the whipping components. In order to examine the validity of the assumption, the rainflow algorithm[13] is applied to the exact stress time histories. In most cases, the cumulative damage per a cycle of wave encounter thus calculated is only 10 to 20 percent larger than the values given by the proposed simple method, while the increase is exceptionally 100 percent for the most significant case of whipping illustrated in Fig. 11. It should be pointed out that the increases of the maximum sagging and maximum hogging bending stresses due to the superposition of wave and whipping components are essential to the reduction of fatigue strength of structural members.

A stress range is obtained from the bending moment divided by the section modulus for an arbitrary location along the ship length. Taking the nominal stress range as the one obtained at S.S. 3–1/2, the fatigue damage per a cycle of wave encounter, D_e, is calculated by parametrically changing stress concentration factors. Since the tensile residual stress is assumed to be 10kgf/mm^2 in the present analysis, the S–N curves are interporated in order to represent the appropriate mean stress conditions. The fatigue damage per a cycle of wave encounter of the wave height 8m is illustrated in Fig. 14, where the stress concentration factors are set as 2.0, 2.5, 3.0 and 3.5, and the S–N curves used are the ones for gas cut surface. It is recongnized that the fatigue damage per a cycle

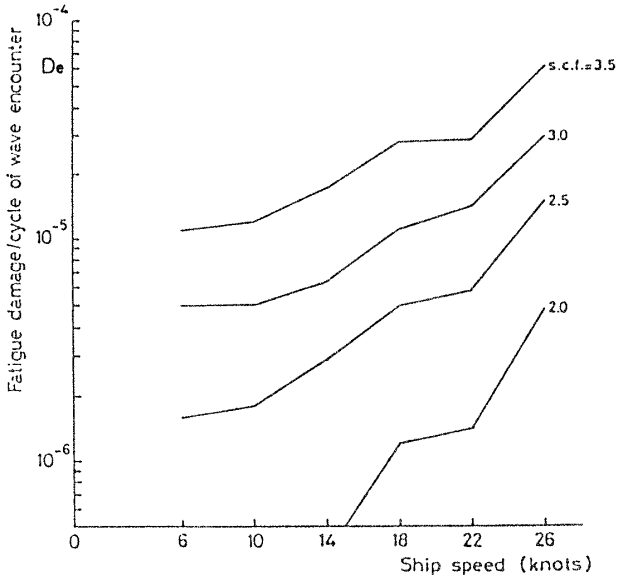

Fig. 14 Fatigue damage per a cycle of wave encounter (H_w=8.0m, gas cut surface)

of wave encounter logarithmically increases with the increase of the ship speed. Figure 15 shows the case for the wave height 10m, where the critical speed U_c is indicated at the ship speed 18knots, above which the fatigue damage drastically increases. If the total number of cycles of this level is of the order of 10^4, fatigue cracks may be initiated in the structural members with the stress concentration factors

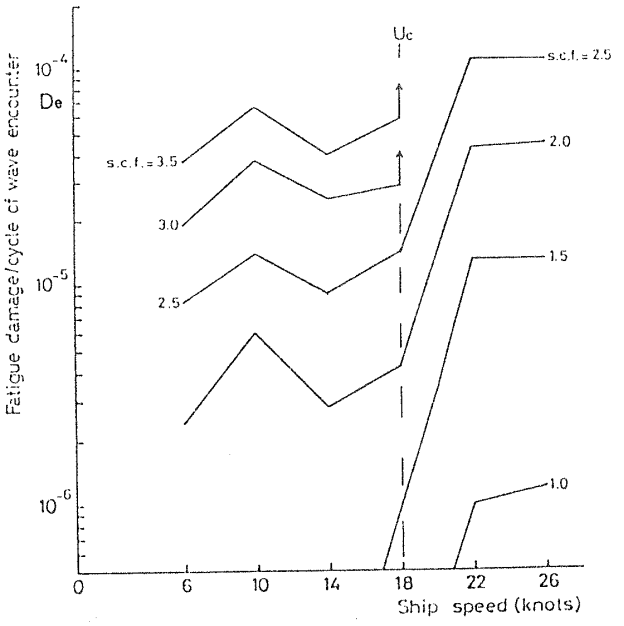

Fig. 15 Fatigue damage per a cycle of wave encounter (H_w=10.0m, gas cut surface)

more than three. Figure 16 shows the case for the cross-shaped fillet weld loaded perpendicular to the weld direction. The results given in Fig. 16 represent relatively low fatigue strength even for lower stress concentration factors in comparison with the ones for gas cut surface.

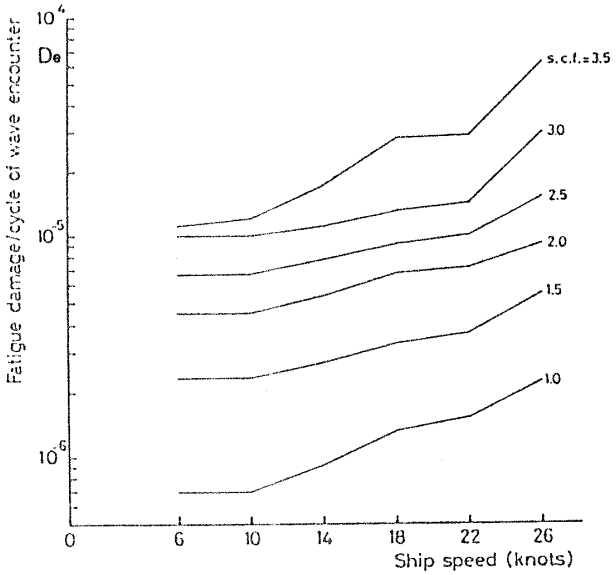

Fig. 16 Fatigue damage per a cycle of wave encounter (H_w=8.0m, cross-shaped fillet weld loaded perpendicular to weld direction)

3.2 A tentave study on the relation between the fatigue strength and ship speed

Since the linear superposition cannot be applied to nonlinear response analysis, the present approach faces difficulties in the estimate of the fatigue damage of actual ships, which go through irregular seas in various heading angles during their whole lives. A tentative study is presented on the relation between the fatigue strength and the ship speed based on very simplified assumptions described below:

(1) The fatigue damage responsible for the fatigue crack initiation is accumulated in the short term sea states of the characteristic wave height more than 6m, where slamming and whipping could occur.

(2) Considering a Japanese container ship in North American service, the severe sea states

which cause slamming and whipping, are expected during her voyages to west in winter. The total days in such conditions are 10 days per a year at most, which are equivalent to the number of cycles of the order of 10^5.

(3) The probability, P_S, of the occurrence of slamming followed by whipping per a cycle of wave encounter in irregular seas is estimated from the data given by Ochi[14], in which ship speed is normalized by Froude number (see Fig. 17).

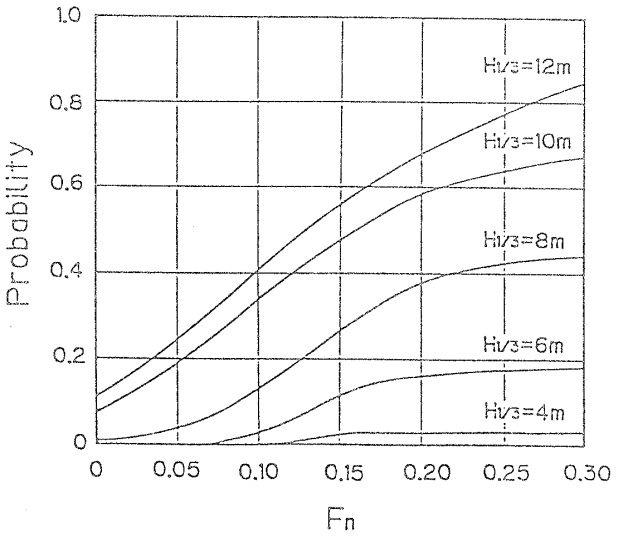

Fig. 17 Probability of occurrence of slam per a cycle of wave encounter in head seas (Mariner type ship ; see Ref. [14])

(4) When slamming occurs in irregular seas, fatigue damage per a cycle of wave encounter is accumulated. The fatigue damage D_e is assumed to be identical to the one in the regular wave, whose wave height is equal to the significant wave height, and whose wave length–ship length ratio is unity.

(5) Fatigue life is calculated as $T_e/(D_eP_s)$ for a given significant wave height, ship speed, and stress concentration factor, where T_e is an average period of wave encounter.

Based on the above assumptions, the relation between significant wave heights, ship speeds, and stress concentration factors are determined for a given fatigue life. Figure 18 illustrates an example of the fatigue damage prediction for gas cut surface, in which the fatigue life is set equal to one year. If the ship is kept to be operated in the lower left region with respect to the curves dependent on the stress concentration factor, fatigue cracks may not be initiated at the structural members.

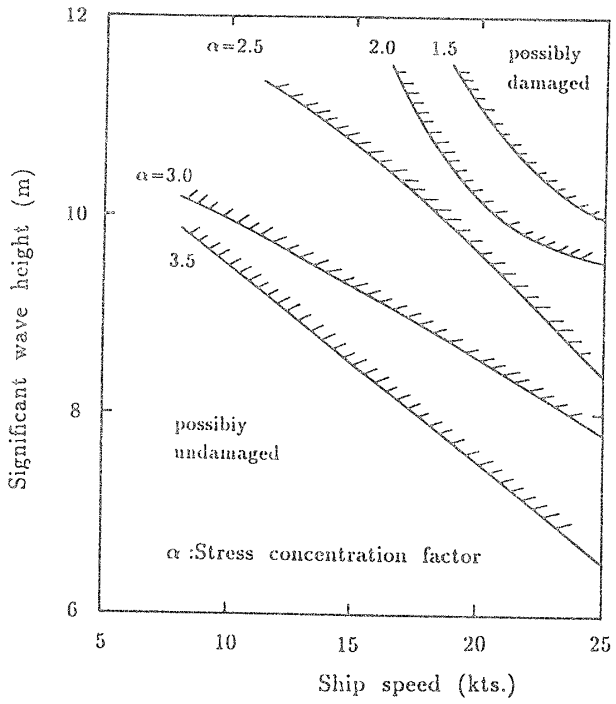

Fig. 18 Prediction of possible fatigue damage for a period of one year in relation to wave heights, stress concentration factors, and ship speeds.

4. Conclusions

It has recently been well recognized that the effects of the nonlinear wave forces significantly increase the sagging moment in the fore body of a hull girder. Considering the whipping effects in the present paper, it should be emphasized that the hogging moment is also increased with ship speeds, and that the both bending moments are increased even in the aft body. Based on the calculated bending stresses and the S–N data for structural components, the fatigue damage per a cycle of wave encounter is found to be logarithmically increased with ship speed. A tentative study is presented for the prevention of fatigue failures for a given service period, which is based on simplified relations among significant wave heights, ship speeds, and stress concentration factors. It is also learned from the present study that the

detailed structural design which reduces stress concentration factors is essential for the prevention of fatigue failures.

Acknowledgement

The authors are grateful to Mr. H. Inoue of Ship Research Institute, Ministry of Transport for instructive discussion on the low-cycle fatigue damage, and also to Kobe Shipyard and Engine Works, Mitsubishi Heavy Industries, Ltd., for providing useful information. Numerical computation was carried out by HITAC M240H at the Information Processing Center of Yokohama National University.

Reference

1) Report of Technical Committee on the Onomichi-Maru Disaster, Ministry of Transport, 1981.
2) Y. Yamamoto, M. Fujino, H. Ohtsubo, T. Fukasawa, Y. Iwai, G. Aoki, I. Watanabe, H. Ikeda, A. Kumano, and T. Kuroiwa, "Disastrous Damage of a Bulk Carrier due to Slamming," Journal of the Society of Naval Architects of Japan, Vol. 154, 1983, pp. 516-524.
3) Y. Yamamoto, K. Iida, T. Fukasawa, T. Murakami, M. Arai, and A. Ando, "Analysis of Structural Damages of the Fore Body of a Container Ship due to Slamming," Journal of the Society of Naval Architects of Japan, Vol. 155, 1984, pp. 246-256.
4) Damage of Shell Plating of Ship Bow due to Waves and the Counterplan for Damage Prevention, Technical Committee Report, Vol. 18, The West-Japan Society of Naval Architects, 1987.
5) Y. Minami, T. Ogawa, and M. Kimura, "Low-Cycle Corrosion-Fatigue Accompanied with Intermittent Impact (First Report)," Journal of the Society of Naval Architects of Japan, Vol. 130, 1971, pp. 321-327.
6) H. Inoue and H. Maenaka, "Experiments on Low-Cycle Fatigue and Fracture Strength of Buckled Members," Proceedings of the Special Conference of the Research and Development on the Disaster Prevention System at Seas, Ministry of Transport, 1987.
7) Vibration Control in Ships, VERITEC, 1985, Norway.
8) H. Ohtsubo, T. Kuroiwa, and Y. Yamamoto, "Structural Response of Ships among Rough Seas (First Report)," Journal of the Society of Naval Architects of Japan, Vol. 157, 1985, pp. 391-402.
9) Y. Yamamoto, M. Fujino, and T. Fukasawa, "Motion and Longitudinal Strength of a Ship in Head Sea and the Effects of Non-Linearities (Third Report)," Journal of the Society of Naval Architects of Japan, Vol. 145, 1979, pp. 63-70.
10) Seakeeping Performance of High Speed Container Ships, Reports of the 125th Research Committee, The Shipbuilding Research Association of Japan, 1972, 1973.
11) T. Kuroiwa and H. Ohtsubo, "Nonlinearity of Sagging Moment of Fine Ships," Journal of the Society of Naval Architects of Japan, Vol. 161, 1987, pp. 234-241.
12) Monograph on Fatigue Strength of Weld, Section 1, Svetskommissionen Ingeniorsvetenskapsakademien, Royal Swedish Academy of Engineering Sciences, Stockholm, 1969.
13) T. Endo and H. Anzai, "Refined Rainflow Algorithm : P/V Difference Method," Journal of the Society of Materials Science, Japan, Vol. 30, No. 328, 1981, pp. 89-93.
14) M. K. Ochi, "Extreme Behavior of a Ship in Rough Seas : Slamming and Shipping of Green Water," Transactions of the Society of Naval Architects and Marine Engineers, Vol. 72, 1964, pp. 143-202.